объединенный
институт
ядерных
исследований
дубна

E4-83-368

R.G.Nazmitdinov*, G.Saupe, K.V.Shitikova**

APPLICATION OF THE METHOD OF HYPERSPHERICAL FUNCTIONS TO DESCRIPTION OF $^{16}O + ^{16}O$ ELASTIC SCATTERING

Submitted to "ЯФ"

* Tashkent State University
** Moscow State University

1983

1. INTRODUCTION

To describe the reactions with heavy ions, at present the theoretical approaches are intensively developed in which the interaction potential is constructed on the basis of the data on effective nucleon-nucleon forces and on distribution of matter in the projectile and in the target. Two of the most popular methods for constructing the nuclear interaction potential (NIP) of heavy ions are the double folding potentials [1] and the energy-density formalism [2]. These approaches make it possible to allow for the effects of nuclear saturation and antisymmetrization [1,3] in the density dependence of interaction forces [4] due to inclusion of nucleon exchange. However, in general the calculations involve various approximations. The imaginary part of NIP, which includes the relevance to various reaction channels, is approximated by the Woods-Saxon phenomenological potential [1], the interacting ion densities are simulated by all the possible functions [4], etc. Among the consistent microscopic scheme for constructing NIP, we feel it necessary to mention the works of Fassler's group [5,6], where an attempt was made to use the G-matrix in order to calculate the imaginary and the real part of the optical potential (OP) of heavy ions on the basis of the properties of infinite nuclear matter.

The formalism of the method of hyperspherical functions (MHF) was used in [7] to obtain the nuclear density distributions for a number of light nuclei (^{4}He, ^{6}Li, ^{12}C, ^{16}O) verified on the basis of sets of experimental data, such as binding energy, monopole resonance excitation energy, r.m.s. nuclear radius, elastic and inelastic form factors for the excitation of monopole resonances [8]. In work [10], the nuclear interaction potentials using finite-range forces proposed by Satchler and Love for systems with $A = 4,6,12,16$ were constructed by parametrizing these densities in the form of two Gaussoids with different parameters [9]. In work [13], the densities obtained in MHF were used to construct not only diagonal but also nondiagonal matrix elements of the potential for monopole excited states of nuclei [11,12] with Skyrme δ-forces. A good agreement with experiment in describing elastic scattering process was obtained in ref. [14] by representing the real and imaginary parts of OP in terms of such a microscopic potential and varying only the renormalization factor for the imaginary part. Besides that, the method of coupled channels was used to calculate the inelastic cross sections of ion interaction involving excitation of monopole giant resonances [15]. These cross sections are also proved to be in an adequate agreement with experimental data for the inelastic scattering process with excitation of 0^+ state in the $^3He + ^{12}C$ reaction. Such studies are urgent because of the numerous experiments carried out in the recent years to find and identify the monopole giant resonances in nuclei. However, the problem of the existence of monopole resonances in light nuclei ($A \leq 16$) has not been solved unambiguously. On the other hand, MHF can give reliable theoretical predictions for the description of monopole oscillations and may be used to study inelastic processes in ion reactions involving excitation of the monopole degree of freedom. In this case, the test of the potentials obtained in MHF by describing elastic scattering of ions is a necessary intermediate stage.

In the present work, the $^{16}O + ^{16}O$ elastic scattering is studied theoretically at different bombarding energies of ions using the nuclear interaction potentials calculated with the densities obtained in terms of MHF. The stability of calculated results with respect to the choice of the model for the construction of the potential [1,2] is analyzed. In the case of the double-folding potential various effective interactions are used, namely finite-range forces suggested by Satchler and Love [10] and Skyrme δ-forces [13] to study the influence of the character of the forces on the behaviour of elastic scattering cross sections.

2. CALCULATION TECHNIQUE

In this section, we shall discuss the scheme of calculating the nuclear interaction potential in ion reactions.

The interaction potential between two nuclei or ions is not completely determined and therefore, the optical model was used to construct the potential for a system of two nuclei $a + A$. The complete wave function of the system $a + A$ is expanded in internal wave eigenfunctions of individual nuclei:

$$\Psi = \Sigma\, \phi_{ai}\, \phi_{Aj}\, \chi_{ij}(R), \tag{1}$$

where $\chi_{ij}(R)$ described the relative motion of the system $a + A$ when nucleus a is in state i and nucleus A is in state j. Elastic scattering corresponds to the wave function $\chi_{00}(R)$. If one neglects the effects of antisymmetrization between two nuclei whose wave functions are separately antisymmetrized, then, according to Feschbach [16], the effective potential of optical model will take the form

$$U_{op} = V_{00} + \sum_{\alpha\alpha'} V_{0\alpha} \left(\frac{1}{E - H + i\epsilon}\right)_{\alpha\alpha'} V_{\alpha' 0} = U_F + \Delta U, \tag{2}$$

where V is the interaction between a and A; the summation runs over all the excited states of one nucleus or both. The first term is the real double-folding potential

$$U_F(R) = V_{00} \equiv (\phi_{a0}\, \phi_{A0}\, |V|\, \phi_{a0}\, \phi_{A0}). \tag{3}$$

The integration in (3) is over all internal coordinates of the two nuclei. The remaining term ΔU, which contains the coupling to the inelastic channels, is of the dynamic nature, so that one has to know the total excitation spectrum of the colliding nuclei in order to construct it. In phenomenological approaches, U_{op} is approximated by the local complex potential U(R), which is used for example, in the Woods-Saxon form. The parameters of the real and imaginary part of OP are often chosen to be independent. Therefore, the radius of the imaginary part of OP is in most cases larger than the radius of the real part.

(a) The Double-Folding Model

When $U_F(R)$ (formula (3)) is calculated by the method of double folding, the densities of the colliding nuclei a and A are assumed to be nondisturbed, and the interaction potential is the mean value of the nucleon-nucleon interaction averaged over two densities:

$$U_{A_1 A_2}(\vec{R}) = \iint \rho_{A_1}(\vec{r}_1)\, \rho_{A_2}(\vec{r}_2) V(|\vec{r}_1 + \vec{R} - \vec{r}_2|)\, d\vec{r}_1\, d\vec{r}_2 . \tag{4}$$

Such a determination seems to be justified at the ion collision energies considered here ($\lesssim$ 10 MeV/nucleon) because the elastic scattering of ions is only sensitive to the form of the potential at a distance between the ions near the radius of strong absorption

$$R_{crit} = 1.5(A_1^{1/3} + A_2^{1/3}). \tag{5}$$

The overlap of the densities of colliding nuclei is small in this region, so that one can assume their distortion to be negligible in this case. For even-even nuclei with $N = Z$, the nucleon-nucleon potential in formula (4) may be assumed to be independent of spin-isospin interaction. Then, using the Skyrme interaction with δ-forces as nucleon-nucleon interaction, we obtain the following double folding interaction potential for the nuclei a and A:

$$U^{a,A}_{ij,k\ell}(R) = \pi \int_0^\pi \sin\Theta\, d\Theta \{ \frac{3}{8} t_0 [\int_0^\infty n^a_{ij}(r) n^A_{k\ell}(|\vec{R}-\vec{r}|) r^2 dr + \int_0^\infty n^A_{ij}(r) n^a_{k\ell}(|\vec{R}-\vec{r}|) r^2 dr] + \frac{t_3}{16} [\int_0^\infty (n^a_{ij}(r))^2 n^A_{k\ell}(|\vec{R}-\vec{r}|) r^2 dr + \int_0^\infty (n^A_{ij}(r))^2 n^a_{k\ell}(|\vec{R}-\vec{r}|) r^2 dr] \}, \quad (6)$$

where $|\vec{R}-\vec{r}| = \sqrt{R^2 + r^2 - 2Rr\cos\Theta}$; t_0, t_3 are the parameters of the two-particle and three-particle Skyrme interaction, respectively; $n_{ij}(r)$ is the density distribution of nuclear matter given by

$$n^A_{ij}(r) = \frac{16}{\sqrt{\pi}} \frac{\Gamma(\frac{5A-11}{2})}{\Gamma(\frac{5A-14}{2})} \int_r^\infty \frac{(\rho^2 - r^2)^{\frac{5A-16}{2}}}{\rho^{5A-13}} \chi_i(\rho)\chi_j(\rho)\, d\rho + \frac{8}{3} \frac{(A-4)}{\sqrt{\pi}} \frac{\Gamma(\frac{5A-11}{2})}{\Gamma(\frac{5A-16}{2})} \int_r^\infty \frac{r^2(\rho^2 - r^2)^{\frac{5A-15}{2}}}{\rho^{5A-13}} \chi_i(\rho)\chi_j(\rho)\, d\rho. \quad (7)$$

The normalization condition is of the form

$$4\pi \int n_{ij}(r) r^2 dr = A,$$

and the r.m.s. nuclear radius is expressed by the relation

$$\overline{R^2_{ii}} = \langle r^2 \rangle_{ii} = \frac{\int n_{ii}(r) r^4 dr}{\int n_{ii}(r) r^2 dr}. \quad (8a)$$

In the case of finite-range forces, the nucleon interaction potential is chosen to be of the Gaussian form allowing for a soft core in the effective interaction at small distances [10]:

$$U(r) = \sum_{k=1}^{2} U_k \exp(-\frac{r^2}{a_k^2}), \quad (9)$$

$$r = |\vec{r}_1 + \vec{R} - \vec{r}_2|.$$

In this case, the Gaussian form with the parameters found from the condition for the best representation of nuclear densities obtained in terms of MHF is also applied to the nuclear matter density distribution. Use is made as a rule of different parameters of the Gaussoids in formula (9), which permits one to describe the asymptotic behaviour of the density correctly. In the language of the shell model this means an effective allowance for mixing of configurations from different shells. Thus, using the following form for the densities of colliding nuclei,

$$\rho_A(r) = \rho_{0A} [\exp(-\frac{r^2}{b^2_{0A}}) + C_1 \frac{r^2}{b^2_{2A}} \exp(-\frac{r^2}{b^2_{2A}})],$$

$$\rho_a(r) = \rho_{0a} [\exp(-\frac{r^2}{b^2_{0a}}) + C_2 \frac{r^2}{b^2_{2a}} \exp(-\frac{r^2}{b^2_{2a}})], \quad (10)$$

we get for the nuclear interaction potential [10]

$$U^{a,A}(R) = \sum_k B_k \{ f_{k0a,0A}(R) \exp(-\frac{R^2}{\delta^2_{k0a,0A}}) + f_{k0a,2A}(R) \exp(-\frac{R^2}{\delta^2_{k0a,2A}}) + f_{k2a,0A}(R) \exp(-\frac{R^2}{\delta^2_{k2a,0A}}) + f_{k2a,2A}(R) \exp(-\frac{R^2}{\delta^2_{k2a,2A}}) \}, \quad (11)$$

where

$$f_{k0a,0A} = \frac{b^3_{0a} b_{0A}}{\delta^3_{k0a,0A}},$$

$$f_{k0a,2A} = C_1 \frac{b^3_{0A} b^3_{2A}}{\delta_{k0a,2A}} (\frac{3}{2} \frac{\mu^2_{k0a}}{\delta^2_{k0a,2A}} + \frac{b^2_{2A}}{\delta^2_{k0a,2A}} \frac{R^2}{\delta^2_{k0a,2A}}),$$

$$f_{k2a,0A} = C_2 \frac{b_{2A}^3 b_{0A}^3}{\delta_{k2a,0A}^3}\left(\frac{3}{2}\frac{\mu_{k0A}^2}{\delta_{k2a,0A}^2} + \frac{b_{2a}^2}{\delta_{k2a,0A}^2}\cdot\frac{R^2}{\delta_{k2a,0A}^2}\right),$$

$$f_{k2a,2A} = C_1 C_2 \frac{b_{2a}^3 b_{2A}^3}{\delta_{k2a,2A}^3}\Big\{\frac{9}{4}\frac{a_k^2}{\delta_{k2a,2A}^2}\left(1 + \frac{5}{3}\frac{b_{2a}^2 b_{2A}^2}{a_k^2 \delta_{k2a,2A}^2}\right) + \left[\frac{3}{2}\frac{b_{2a}^2}{\mu_{k2a}^2}\left(1 + \frac{a_k^2 b_{2A}^2}{b_{2a}^2 \delta_{k2a,2A}^2}\right) - 5\frac{b_{2a}^2 b_{2A}^2}{\delta_{k2a,2A}^4}\right]\frac{R^2}{\delta_{k2a,2A}^2} + \frac{b_{2a}^2 b_{2A}^2}{\delta_{k2a,2A}^8} R^4\Big\}. \quad (12)$$

$$B_k = \pi^3 \rho_{0a}\rho_{0A} V_k a_k^3,$$

$$\delta_{kma,nA} = \sqrt{a_k^2 + b_{ma}^2 + b_{nA}^2},$$

$$\mu_{kns} = \sqrt{a_k^2 + b_{ns}^2}.$$

In the case of heavy ion interaction we use the zero-range pseudopotential [1]

$$U_\delta(r) = dE\delta(r) \quad (13)$$

in order to take into account the Pauli principle effectively. This correction term depends on the mass number of the system and the incident energy in the following way:

$$d(E) = -276\left(1 - 0{,}005\frac{E}{A}\right)\ \text{MeV fm}^3. \quad (14)$$

(b) The Energy-Density Formalism

In this case, NIP between two ions is calculated in the sudden approximation, where it is assumed that the ion densities are frozen at the moment of collision. Then, NIP takes the form

$$U(R) = \int \{\epsilon(\rho_a + \rho_A) - \epsilon(\rho_a) - \epsilon(\rho_A)\}dr, \quad (15)$$

where $\epsilon(\rho)$ is the energy density for the relevant system which is determined as [2]

$$\epsilon(\rho) = \tau_{TF} + \rho V(\rho,\alpha) + \eta_0(\nabla\rho)^2 + \frac{1}{2}e\rho_p V_e - 0.378e^2\rho_p^{4/3}, \quad (16)$$

where $\rho = \rho_n + \rho_p$; ρ_n (ρ_p) is the density of the neutron (proton) component in the nucleus; α is the neutron excess

$$\alpha = \frac{\rho_n - \rho_p}{\rho_n + \rho_p}. \quad (17)$$

The first term in (16) is the density of the kinetic energy due to the Thomas-Fermi approximation

$$\tau_{TF} = a_k\rho^{5/3} = \frac{3}{5}\frac{\hbar^2}{2m}\left(\frac{3}{2}\pi^2\right)^{2/3}\frac{1}{2}[(1-\alpha)^{5/3} + (1+\alpha)^{5/3}]\rho^{5/3}, \quad (18)$$

where m is nucleon mass. The functional $V(\rho,\alpha)$ corresponds to the potential energy of a particle in nuclear matter

$$V(\rho,\alpha) = b_1(1 + a_1\alpha^2)\rho + b_2(1 + a_2\alpha^2)\rho^{4/3} + b_3(1 + a_3\alpha^2)\rho^{5/3}. \quad (19)$$

The gradient term in (16) arises from the finiteness of the nuclear system, the two last terms correspond to the direct and exchange Coulomb energies. The values {a, b} are determined by fitting the binding energy and the proton radius. It should be noted that NIP was calculated in the energy-density formalism using the same densities (formula (10)) as in the case of the finite-range potential.

In the case of $^{16}O + ^{16}O$ system, the parameter $\alpha = 0$ and the density parameters in $\rho_A(r)$ and $\rho_a(r)$ are also the same. Considering the latter, we obtain for NIP:

$$U(R) = 2\pi\int_{-1}^{1} d\cos\Theta \int_0^\infty f(R,\Theta,r)\,r^2 dr,$$

$$f(R,\Theta,r) = \tilde{\epsilon}(\rho_a + \rho_A) - \tilde{\epsilon}(\rho_a) - \tilde{\epsilon}(\rho_A) - 2\eta_0 f_1, \quad (20)$$

$$f_1 = (4r^2 - R^2\cos^2\Theta)C_a C_A,$$

$$C_{a(A)} = -\frac{\rho_{0A}}{b_{0a}^2}\exp\left(-\frac{r_{a(A)}^2}{b_{0a}^2}\right) + \frac{C_2}{b_{2a}^2}\exp\left(-\frac{r_{a(A)}^2}{b_{2a}^2}\right)(b_{2a}^2 - r_{a(A)}^2),$$

$$|\vec{r}_a| = \sqrt{r^2 + \frac{1}{4}R^2 - \frac{1}{2}rR\cos\Theta}, \quad |\vec{r}_A| = \sqrt{r^2 + \frac{1}{4}R^2 + \frac{1}{2}rR\cos\Theta},$$

where R is the distance between ion centers; $\tilde{\varepsilon}(\rho)$ is the corresponding functional (16) without the gradient term. When deriving formula (20), we disregarded the contribution from the direct Coulomb term for it is included effectively in the computation of the cross sections.

(c) Cross Sections of Elastic Scattering

The angular distributions for elastic scattering of ions were calculated using programs TUFO and CHUCK. It was assumed that the forms of the real and imaginary potentials were the same, so that

$$U = U_{00,00} \quad (1 + i\chi_{00,00}). \tag{21}$$

The factor $\chi_{00,00}$ in the elastic channel was found by fitting theoretical differential cross sections to experimental data. The criterion of fitting is the usual one, namely, we minimized the value

$$\chi^2 = \sum_i \left[\frac{\sigma_{exp}(\Theta_i) - \sigma_{theor.}(\Theta_i)}{\Delta\sigma_{exp}(\Theta_i)} \right]^2 , \tag{22}$$

where $\sigma_{theor.}(\Theta_i)$ are the calculated differential cross sections; $\sigma_{exp}(\Theta_i)$ are the measured cross sections; $\Delta\sigma_{exp}(\Theta_i)$ are the experimental errors.

3. CALCULATED RESULTS AND DISCUSSION

The nuclear interaction potentials of two ions are determined by the form of effective nucleon-nucleon interaction and by the distribution of matter in them. Figure 1 shows the density of ^{16}O nucleus calculated by MHF for two versions of the nucleon-nucleon interaction (Brink-Boeker potential [17]). If the parameter set B4 is used, we obtain a narrower density distribution, but with a more clearly expressed maximum for R = 1,2fm compared with the result given by the parameter set B1. The use of the parameter set B1 gives rise to a larger nuclear radius. Obviously, the use of different nucleon-nucleon interaction potentials in MHF leading to different nuclear density distributions must affect the results of calculations of NIP of two ions.

Figure 2 shows the results of calculation of NIP in the double folding method with the Skyrme interaction [13] for three sets of parameters t_0 and t_3. The values of the parameters are presented in Table 1. Versions (a), (b), (c) differ by the three-particle force contribution determined by the parameter t_3.

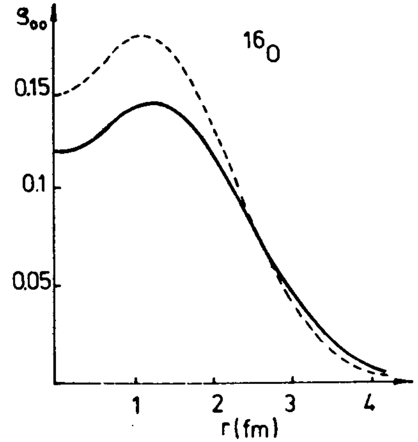

Fig.1. Density distribution of the ground state of ^{16}O nucleus for the potentials B1 (——) and B4 (----).

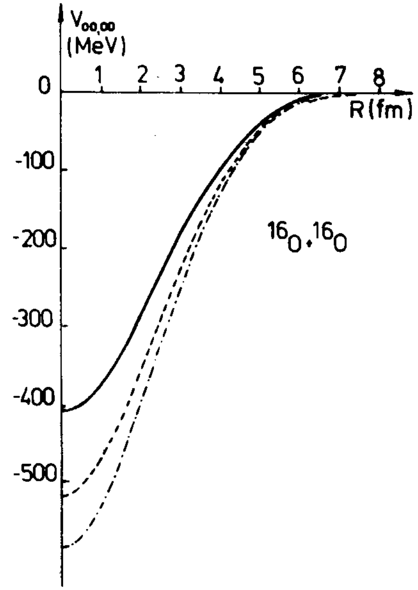

Fig.2. Double-folding potential of $^{16}O + ^{16}O$ with Skyrme forces for three sets of parameters t_0, t_3 from Table 1 (a ———, b ------, c —· ——).

As the ratio $|t_0/t_3|$ rises, the calculated potential gets deeper. Thus, an increase in the contribution of the three-particle forces, which are of repulsive nature, gives rise to a decrease in NIP depth. Figure 3 shows the results for the $^{16}O + ^{16}O$ NIP computed in the energy-density formalism (dots), by the double-folding method with the Skyrme forces (the solid line corresponds to NIP calculated with the densities obtained in MHF with the set of parameters B1, and the dashed line with B4), and with finite-range forces allowing effectively for ($d \neq 0$, the dot-dash line) and disregarding ($d = 0$, two dots-

Table 1

	t_0	t_3	$\lvert t_0/t_3 \rvert$	V(MeV) at R = 0.1 fm
a)	-1057.3	14464.4	0.073	-410.25
b)	-1170.0	9331.0	0.125	-522.75
c)	-1205.6	5000.0	0.241	-586.20

dash line) anti-symmetrization. Table 2 presents the parameters of the potential calculated in the energy-density formalism.

Table 2

b_1	b_2	b_3	a_1	a_2	a_3	η_0
-588.75	563.56	160.92	-0.424	-0.0973	-2.25	7.23

The parameters of the potentials obtained by the double-folding method with finite-range forces are presented in Table 3.

Table 3

Version of forces	V_1(MeV)	V_2(MeV)	a_1(fm)	a_2(fm)	d (MeV fm^3)
1	553.18	1781.4	0.8	0.5	0
2	601.99	2256.4	0.8	0.5	$-276(1-0.005\frac{E}{A})$

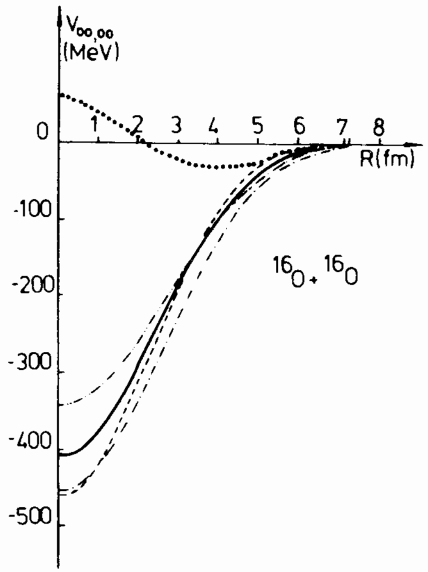

Fig.3. Potential of $^{16}O+^{16}O$ in the energy-density formalism (....), in the double-folding method with Skyrme forces: B1 (——), B4 (---); with Satchler-Love forces including (——· ——) and disregarding (—— ··——) antisymmetrization.

The calculations have shown that the interaction potential depth is determined by the density distributions of colliding ions, namely an increase in the density at small distances for the set B4 compared with the set B1 (see Fig.2) results in a deepening of NIP. The NIP calculated in the double-folding method with finite-range forces is characterized by a stronger interaction at high R compared with the result obtained using the δ-force. In particular, the values of the NIP at the critical radius are $V(R_{crit.}) = -1.05$ MeV for the parameter set B1 and Skyrme-forces (version (a), Table 1) and $V(R_{crit.}) = -2.74$ MeV in the case of finite-range forces. The consideration of the antisymmetrization effect in the calculations with the finite-range forces results in a deeper potential at all values of R. The NIP obtained in the energy-density formalism is characterized by a repulsive core up to R = 2.2 fm. Its maximum depth $V_0 = -31.35$ MeV at R = 4.1 fm is much smaller than in other cases. Thus, the $^{16}O+^{16}O$ interaction potentials calculated by using various models [1,2] with various effective forces are much different at small distances, but these differences become insignificant in the peripheral region.

The calculated NIP were used to analyse the differential cross sections of elastic scattering $^{16}O+^{16}O$ at E_{lab}= 41, 49, 63 MeV [18]. Figure 4 shows differential cross sections calculated using the Skyrme interaction (version (a)) in comparison with experimental data at three energies. The parameter of the imaginary part of the OP was varied depending on the bombarding energy of the ions in order to obtain a better reproduction of experimental data. Its value was found to be $\chi_{00,00}$= 0.04, 0.1, 0.2, respectively. The thin line represents the result of a phenomenological calculation based on the Woods-Saxon potential [18]. At the bombarding energy E_{lab} = 63 MeV the result of the microscopic calculation is in better agreement with experimental data than that given in ref. [18]. In particular, the most realistic description, compared with the phenomenological model, is obtained at small angles. For the lower bombarding energies the differential cross sections are represented only qualitatively.

In the following the effect of the three-particle forces on the differential cross section of elastic scattering was investigated. Figure 5 shows a comparison of the differential cross sections calculated using the Skyrme nucleon-nucleon interaction potential for different sets of parameters (see Table 1 and Fig. 2) with the experimental data obtained at E_{lab} = 63 MeV. The estimates based on χ^2 indicate that the best agreement with the experimental results is obtained for the highest contribution of three-particle forces. In all the cases, a rather good description of experimental data can be obtained at scattering angles up to $\Theta = 65°$ for $\chi_{00,00}$= 0.2.

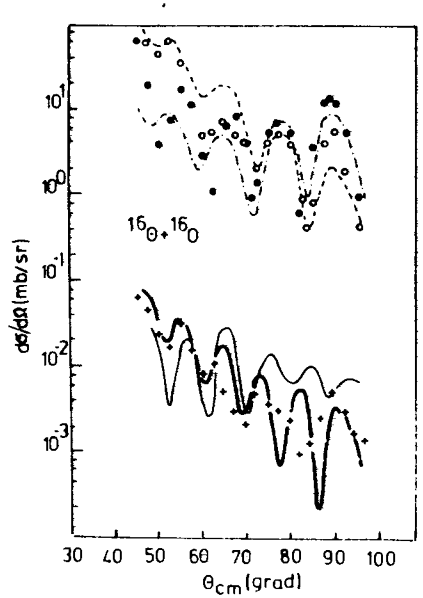

Fig.4. Elastic scattering cross sections calculated with Skyrme forces and the relevant experimental data for E_{lab} = = 41 MeV (—— · ——, O), 49 MeV (---, ●), 63 MeV (——, +).

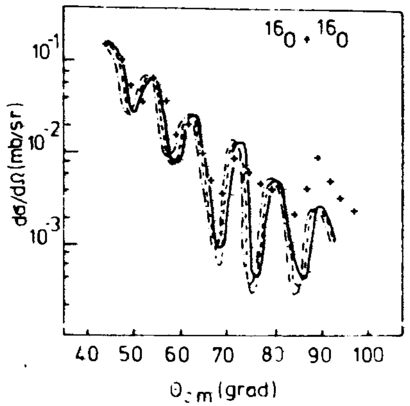

Fig.5. Experimental data on elastic scattering cross sections (+) and the results of calculations for three versions of Skyrme forces ((a) ——) at, (b) --- (c) —·—— E_{lab}= 63 MeV.

Using the NIP with the finite-range forces the differential cross sections for elastic scattering were calculated at E_{lab} = 49,63 MeV, where the parameter of the imaginary part was $\chi_{00,00} = 0.3$. From Fig. 6 it follows that the better description is obtainable at a higher energy. However, the use of the potential with finite-range forces permits a fairly good interpretation of elastic scattering cross sections in a broader interval of angles compared with the previous one also at E_{lab} = 49 MeV. Therefore, this potential allows the most realistic description of the elastic scattering of two ions in comparison with other potential types investigated. Figure 7 shows the results of the calculations with NIP obtained in the energy-density formalism. This potential has a repulsive core and a relatively small depth. In order to describe experimental data we had to introduce two free parameters according to $U = (\alpha + i\beta) U_{00,00}$. A satisfactory agreement can be obtained with $\alpha = 2.7$ and $\beta = 0.3$ for E_{lab} = 49 MeV. However, it is impossible to describe the experiment at E_{lab} = 63 MeV in the interval of scattering angles $\Theta < 80°$.

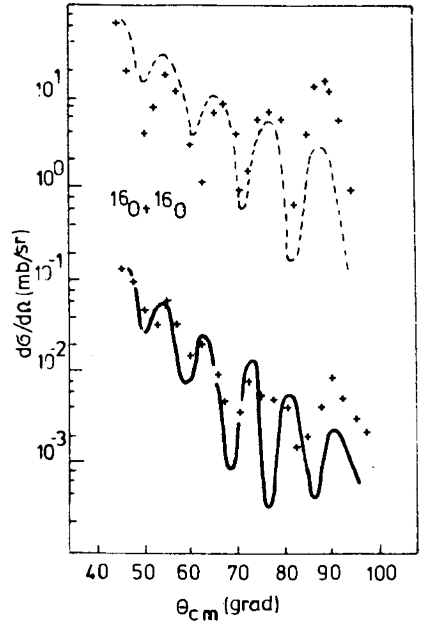

Fig.6. Cross sections of $^{16}O + ^{16}O$ elastic scattering at E_{lab} = 49 MeV (---) and 63 MeV (——) for finite-range forces.

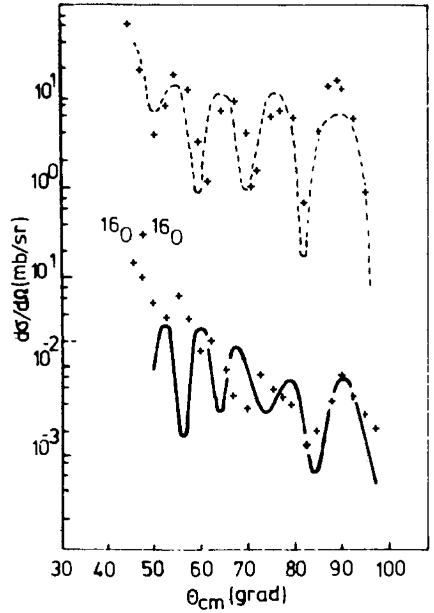

Fig.7. Cross sections of $^{16}O+^{16}O$ elastic scattering at E_{lab} = 49 MeV (---) and 63 MeV (——) for the potential given by the energy-density formalism.

4. CONCLUSION

We used the microscopic nuclear densities obtained in MHF to construct NIP for ^{16}O ions in the double-folding method and in the energy-density formalism. It has been shown that the choice of nucleon-nucleon interaction, when obtaining densities, determines the NIP behaviour at small distances; in the peripheral region this difference is insignificant. Comparatively identical description of elastic scattering by using the realistic NIP on the basis of the finite-range forces and the potential calculated with the Skyrme δ-forces, respectively, indicate that three-particle forces have to be taken into account. Small changes of the NIP depth both in the case of Skyrme δ-forces and for finite-range forces do not lead to marked differences in the descriptions of elastic scattering cross sections. However, the appearance of a repulsive core in NIP gives rise to the necessity of a considerable renormalization of the potential. Therefore, the internal part of NIP may affect the calculated cross sections for the elastic scattering of ions.

It should be noted that, by varying only a single parameter on the imaginary part of the OP we can obtain a comparable (and sometimes a better) description of the differential cross sections for elastic scattering of ^{16}O ions compared with the phenomenological method where up to 6 parameters have to be used, for example in the case of the Woods-Saxon potential.

ACKNOWLEDGEMENT

The authors are indebted to F.A.Gareev and V.M.Shilov for critical remarks and informative discussions of the problems treated in this work.

REFERENCES

1. Satchler G.R., Love W.G. Phys.Lett., 1976, 65B, p. 415; Phys.Rev., 1979, 55, p.3.
2. Lombard R.J. Ann.Phys., 1973, 77, p. 380; Ngo H., Ngo Ch. Nucl.Phys., 1980, A348, p. 140.
3. Panda K.C., Behera B., Satpathy R.K. Journ.Phys., 1981, G7, p. 937.
4. Vinas F.J., Lozano M., Madurga G. Phys.Rev., 1981, C23, p. 780.
5. Izumoto T., Krewald S., Faessler A. Nucl.Phys., 1981, A357, p. 471.
6. Sartor R. et al. Nucl.Phys., 1981, A359, p. 467.
7. Kaschiev M., Shitikova K.V. Yad.Fiz., 1979, 30, p. 1479.
8. Burov V.V. et al. Journ.Phys., 1981, G7, p. 137.
9. Orlova N.V., Shirokova A.A., Shitikova K.V. Abstracts of the XXX Symposium on Nuclear Spectroscopy and Structure of the Atomic Nucleus, Leningrad, 1980, p. 203.
10. Burov V.V. et al. JINR, P4-83-279, Dubna, 1983; Knyazkov O.M., Hefter E.F. Z.Phys., 1981, A301, p. 277; Knyazkov O.M. Yad.Fiz., 1981, 33, p. 1176.
11. Dymarz R., Molina J.L., Shitikova K.V. Z.Phys., 1981, A299, p. 245.
12. Dymarz R., Shitikova K.V. JINR, E7-81-653, Dubna, 1981.
13. Vautherin D., Brink D.M. Phys.Lett., 1970, 32B, p. 149.
14. Demyanova A.S., Shitikova K.V. Yad.Fiz., 1982, 35, p. 1431.
15. Dymarz R., Nazmitdinov R.G., Shitikova K.V. ICOHEPANS, D10, Versailles, 1981, p. 139.
16. Feshbach H. Ann. Phys., 1967, 19, p. 287.
17. Brink D.M., Boeker E. Nucl.Phys., 1967, A91, p. 1.
18. Maher J.V. et al. Phys.Rev., 1969, 188, p. 1665.

Received by Publishing Department
on Juny 3,1983.

SUBJECT CATEGORIES
OF THE JINR PUBLICATIONS

Index	Subject
1.	High energy experimental physics
2.	High energy theoretical physics
3.	Low energy experimental physics
4.	Low energy theoretical physics
5.	Mathematics
6.	Nuclear spectroscopy and radiochemistry
7.	Heavy ion physics
8.	Cryogenics
9.	Accelerators
10.	Automatization of data processing
11.	Computing mathematics and technique
12.	Chemistry
13.	Experimental techniques and methods
14.	Solid state physics. Liquids
15.	Experimental physics of nuclear reactions at low energies
16.	Health physics. Shieldings
17.	Theory of condenced matter
18.	Applied researches
19.	Biophysics

Назмитдинов Р.Г., Саупе Г., Шитикова К.В. E4-83-368
Применение метода гиперсферических функций к описанию упругого рассеяния $^{16}O + ^{16}O$

Рассчитаны потенциалы ядерного взаимодействия для системы $^{16}O + ^{16}O$ в формализмах двойной свертки и плотности энергии на основе радиального распределения плотности этих ядер, полученного методом гиперсферических функций. Исследована зависимость сечения упругого рассеяния в этой системе при различных энергиях от типа нуклон-нуклонных сил, а также проанализирована устойчивость результатов к выбору модели для построения потенциала ядерного взаимодействия.

Работа выполнена в Лаборатории теоретической физики ОИЯИ.

Препринт Объединенного института ядерных исследований. Дубна 1983

Nazmitdinov R.G., Saupe G., Shitikova K.V. E4-83-368
Application of the Method of Hyperspherical Functions to Description of $^{16}O + ^{16}O$ Elastic Scattering

The potentials of nuclear interaction of $^{16}O + ^{16}O$ have been calculated in the framework of the folding model and in the energy-density formalism using the radial density distributions of the nuclei obtained by the method of hyperspherical functions. The dependence of the cross section of the elastic scattering in this system at various incident energies on the type of the nucleon-nucleon forces and the influence of the choice of the model for the nuclear interaction potential on the results have been investigated.

The investigation has been performed at the Laboratory of Theoretical Physics, JINR.

Preprint of the Joint Institute for Nuclear Research. Dubna 1983